Mycoscience 41: 481–489, 2000

Spatial associations between actin filaments, endoplasmic reticula, mitochondria and fungal hyphae in symbiotic cells of orchid protocorms

Yukari Uetake[1)]* and R. Larry Peterson[2)]

[1)] National Grassland Research Institute, Nishinasuno, Tochigi 329–2793, Japan
[2)] Department of Botany, University of Guelph, Guelph, Ontario N1G 2W1, Canada

Accepted for publication 26 June 2000

The relationships between endoplasmic reticula (ER), mitochondria, and actin filaments (Afs) were observed in uncolonized and colonized cells of symbiotic protocorms of *Spiranthes sinensis* (Orchidaceae) germinated in the presence of the fungus, *Ceratobasidium cornigerum*. Mitochondria and ER were observed by transmission electron microscopy, and with the fluorescent probe $DiOC_6$ (3) (3,3′-dihexyloxacarbocyanine) combined with confocal laser scanning microscopy (CLSM). An indirect immunofluorescence method using CLSM and an indirect, pre-embedding immunogold method at the ultrastructural level were used for observation of Afs. In uncolonized cells, cortical ER showed a polygonal pattern and ER formed a network throughout the cytoplasm. In the cortex, a smooth face of ER contacted the plasma membrane. Mitochondria were associated with ER. Afs were in close proximity to ER, mitochondria and amyloplasts. Colonized cells retained cortical ER, and a smooth face of ER was also closely associated with the perifungal membrane. ER and mitochondria were present in the cytoplasmic channels bridging between the central peloton and the peripheral cytoplasm. This distribution of ER and mitochondria during fungal colonization and senescence coincided with that of Afs. The changes in the arrays of Afs accompanying symbiotic fungal colonization and senescence occurred concomitantly with the changes in ER.

Key Words——actin filaments; ER; immunocytochemistry; mitochondria; orchid mycorrhiza.

Fungal invasion of plant cells triggers physiological and structural changes in invaded and contiguous cells (Heath, 1997). The extent of cytological changes depends on the type of plant-fungal interaction, and until recently these have been studied primarily by light microscopy and transmission electron microscopy. With the development of confocal laser scanning microscopy (CLSM), new information is being obtained concerning plant-fungal interactions. For example, microtubules (Mts) and actin filaments (Afs), major components of the cytoskeleton, are modified when plant cells are invaded by fungal hyphae (Hardham and Mitchell, 1998; Peterson et al., 1999). Biotrophic pathogenic fungi have been studied most intensively, and it has been determined that the cytoskeleton is altered differentially depending on whether the interaction between the symbionts is compatible or incompatible (Baluška, et al., 1995; Kobayashi et al., 1994; Kobayashi et al., 1992; Kobayashi et al., 1995; Kobayashi et al., 1997a; Kobayashi et al., 1997b; Škalamera and Heath, 1998).

Mutualistic associations between fungi and plants in which fungal hyphae enter plant cells but are enclosed within a plant cell-derived membrane system (endomycorrhizas) also involve changes in the organization of the cytoskeleton. In arbuscular mycorrhizas (AM), in which Glomalean fungal species interact with roots of the majority of vascular plant species, the cortical arrays of Mts and Afs largely disappear, and populations of both of these cytoskeletal components become associated with the fungal structures that develop within root cortical cells (Bonfante et al., 1996; Genre and Bonfante, 1997, 1998; Matsubara et al., 1999).

We have used symbiotic seed germination and protocorm development *in vitro* of the orchid, *Spiranthes sinensis* (Pers.) Ames colonized by the fungus *Ceratobasidium cornigerum* (Bourdot) Rogers as a model system to study the changes in the subcellular organization of plant cells during the establishment and senescence of a mutualistic symbiosis (Peterson et al., 1998). Profound alterations in both Mts and Afs in colonized plant cells occur during the cycle of establishment and senescence of this association (Uetake et al., 1997; Uetake and Peterson, 1997, 1998). Although some observations of the alterations in other cellular components have been made by transmission electron microscopy (TEM) (Uetake and Peterson, 1997, 1998), the interaction between fungal hyphae, the cytoskeletal system and other subcellular structures has not been studied.

Since Afs have a close association with the endoplasmic reticulum (ER) system in plant cells (Quader et al., 1987; Hepler et al., 1990; Staehelin, 1997; Reuzeau et al., 1997), and both Afs and ER are localized around

* Corresponding author.

fungal hyphae in colonized orchid cells (Uetake and Peterson, 1997), the objectives of this study were to monitor changes in the distribution of ER, mitochondria, and other organelles during the colonization process and to determine the relationship between Afs, ER and other organelles in this system using both TEM and CLSM.

$DiOC_6$ (3) was used to detect mitochondria and ER with CLSM, based both on the findings of Terasaki et al. (1984) that ER could be detected in both fresh and fixed animal tissues using this fluorescent probe, and our own preliminary observations of excellent structural detail of the cortical network of ER using this probe with fresh and fixed onion epidermal cells.

Materials and Methods

Symbiotic plant materials Seeds of the terrestrial orchid *S. sinensis* were surface-sterilized and sown on oat agar medium (0.3% oatmeal, 1.0% agar) in Petri dishes, and a plug of potato dextrose agar with mycelium of *C. cornigerum* (anastomosis group C) was placed in the center of the dish. Petri dishes were incubated at 20°C in the dark and at various times after seed germination developing protocorms of various size were collected and processed for microscopy.

Observations of ER using TEM Symbiotically growing protocorms were fixed with 2.5% glutaraldehyde (GA)–2% paraformaldehyde (PA) in 50 mM cacodylate buffer (pH 7.4) with 5 mM $CaCl_2$ for 2 h at room temperature. The materials were rinsed in buffer, hand-sectioned in half, and the sections were then post-fixed in 2% OsO_4 for 1 h at room temperature. After rinsing with H_2O, the materials were either dehydrated, or block-stained in 2% aqueous uranyl acetate for 2 h and then dehydrated through a graded ethanol series. Tissues were embedded in Spurr's resin through a graded series of the resin using propylene oxide as the transition fluid, and polymerized at 70°C. Ultra-thin sections were cut and observed after post-staining with lead citrate with a JEOL-100CX TEM.

Observations of ER using CLSM Symbiotic protocorms were fixed in 1% GA–4% PA or 2.5% GA–2% PA in PME buffer (50 mM PIPES, 1 mM $MgSO_4$, 2 mM EGTA; pH 7.0) or 50 mM cacodylate buffer (pH 7.4) with 5 mM $CaCl_2$ (CC) at room temperature for several hours to overnight. The protocorms were hand-sectioned in half and stained with 10 μg/ml of $DiOC_6$ (3), (3,3'-dihexyloxacarbocyanine, freshly made from a 2.5 mg/ml of stock solution in ethanol) in H_2O for 5 min. The tissues were immediately observed with a Bio-Rad MRC-600 CLSM interfaced with a Nikon Optiphot-2 microscope. A 60X oil immersion lens was used in combination with PMT detector 2 (< 560 nm emission wavelength). Observations of materials were made within 2 h after staining.

Immunogold labelling of AFs using pre-embedding methods Symbiotically growing protocorms were fixed with 1.0% GA–4% PA in PME for 1 h, rinsed in the buffer 3 times, and hand-sectioned in half with a two-sided razor blade. The tissues were then treated with 0.1% $NaBH_4$ in PBS (50 mM phosphate buffer, 150 mM NaCl, pH 7.0), and rinsed in PBS. After blocking with 1% bovine serum albumin (BSA) in PBS for 30 min, the tissues were treated with a monoclonal mouse anti-actin primary antibody (Amersham International plc, Buckinghamshire, England) diluted 1 : 50 in the BSA solution overnight at 4°C, rinsed in PBS, then blocked with BSA in PBS. They were then incubated with polyclonal goat anti-mouse secondary antibody (Jackson Immuno Research Laboratories, Inc. West Grove, PA, USA) conjugated either with the fluorescent probe Cy3™ for CLSM or with 10 nm gold (diluted 1 : 20 in the blocking solution) for 3 h at room temperature. For CLSM, the confocal microscope and method of image capture as described by Uetake et al. (1997) were used. For TEM, tissues were rinsed in PBS and phosphate buffer (PB), post-fixed in 2.5% GA in PB, and rinsed in distilled water. The protocorm halves were then stained with 2% uranyl acetate in distilled water for 1 h, dehydrated with an ethanol series and infiltrated with Spurr's resin using propylene oxide as a transition fluid. Embedded tissues were polymerized at 70°C. Ultra-thin sections were cut at right angles to the original cut surface, post-stained with lead citrate, then observed with a JEOL 100-CX TEM.

Results

Distribution of ER and other organelles determined by conventional TEM Uncolonized protocorm cells had a central vacuole system and peripheral cytoplasm in which extensive cortical ER with various configurations was located (Fig. 1a). The network of cortical ER had some profiles closely associated with the plasma membrane (Fig. 1a). Cells with intracellular fungal hyphae had ER associated with the perifungal membrane (Fig. 1b); these cells retained the cortical network of ER (Fig. 1c), again with some profiles closely associated with the plasma membrane (Figs. 1c, 1d). Cytoplasmic ER was present also adjacent to the host cell nucleus (Fig. 1c).

Distribution of ER and mitochondria determined by CLSM Uncolonized protocorm cells had a complex, polygonal network of cortical ER immediately adjacent to the plasma membrane (Fig. 2a). A combination of sac-like and tubular profiles of ER was evident at greater depths within the cell and numerous mitochondria were associated with this cytoplasmic network (Fig. 2b). Regions of cells also contained amyloplasts, mitochondria and profiles of ER (Fig. 2c). The host cell nucleus was surrounded by stained material, some of which was ER and some mitochondria (Fig. 2d). Cytoplasmic channels stained intensely and had various organelles including amyloplasts associated with them (Fig. 2d).

Colonized cells had centrally located hyphal coils (pelotons) (Fig. 3a) and, in some cases, clumps of degenerated hyphae (Fig. 3b) with cytoplasmic channels bridging between them and the peripheral cytoplasm of the cell (Figs. 3a, 3b). Profiles of ER ensheathed the hyphae (Fig. 3c), and numerous mitochondria were localized in the cytoplasmic channels (Figs. 3a, 3b) and adjacent to the fungal hyphae (Fig. 3c), with fewer present in the peripheral cytoplasm. Host cell nuclei also were sur-

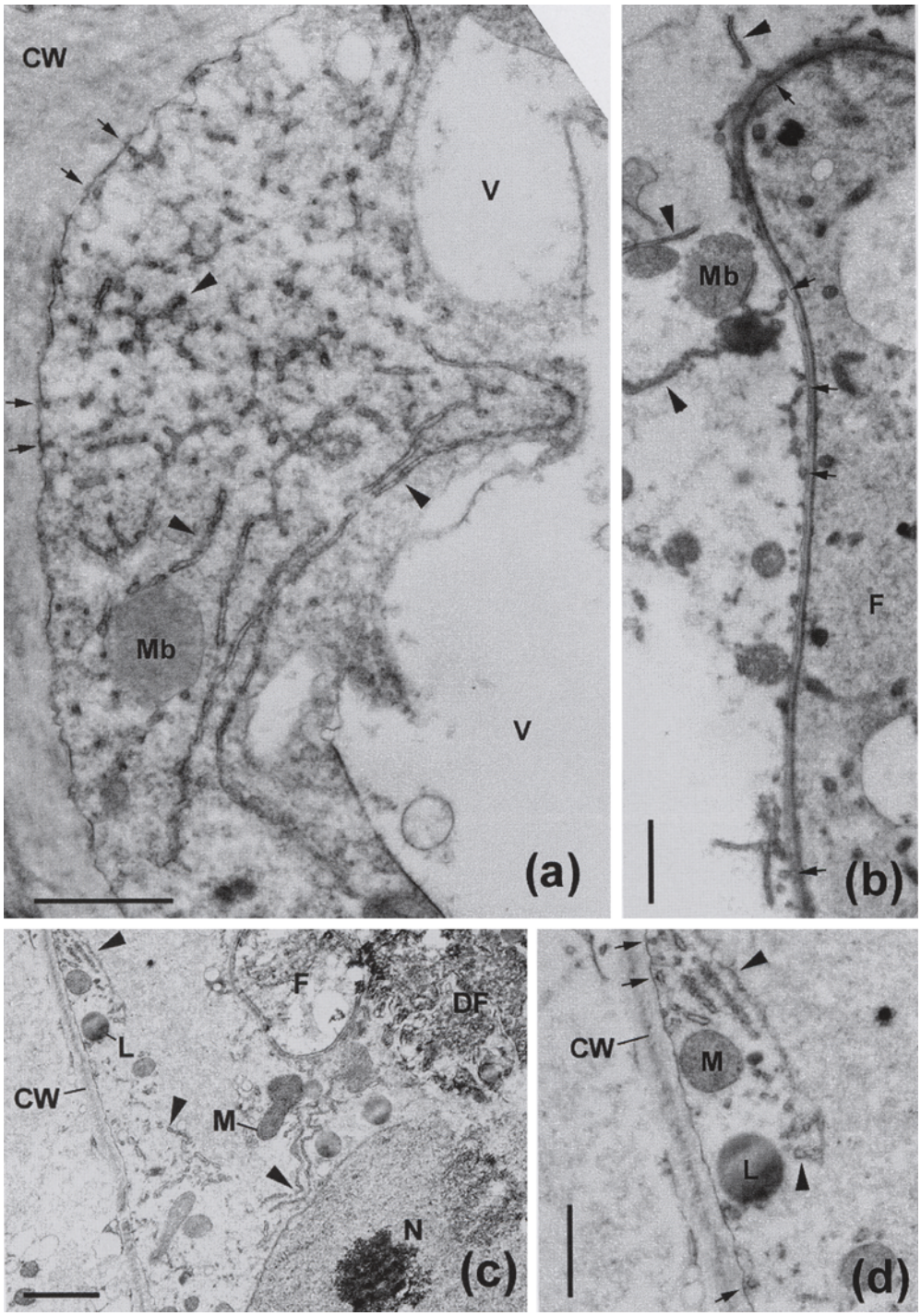

Fig. 1. Cells of symbiotic protocorms of *Spiranthes sinensis* viewed with conventional TEM. (**a**) Cortical region of an uncolonized cell with a central vacuole system (v) and cortical ER (arrowheads). Some ER (arrows) is very close to the plasma membrane. CW=cell wall. Mb=microbody. Bar=1 μm. (**b**) Fungal hypha (F) and adjacent cytoplasm. ER (arrowheads) contacts the perifungal membrane (small arrows). Mb=microbody. Bar=1 μm. (**c**) Colonized cell. A hypha (F) in transverse section and degraded fungal hyphae (DF) are present. ER (arrowheads) is present in the peripheral cytoplasm and adjacent to the host nucleus (N). Lipid bodies (L) and mitochondria (M) are present. CW=cell wall. Bar=2 μm. (**d**) Magnified view of Fig. (c). ER (arrowheads) is very close to the plasma membrane (small arrows). CW=cell wall. L=lipid body. M=mitochondrion. Bar=1 μm.

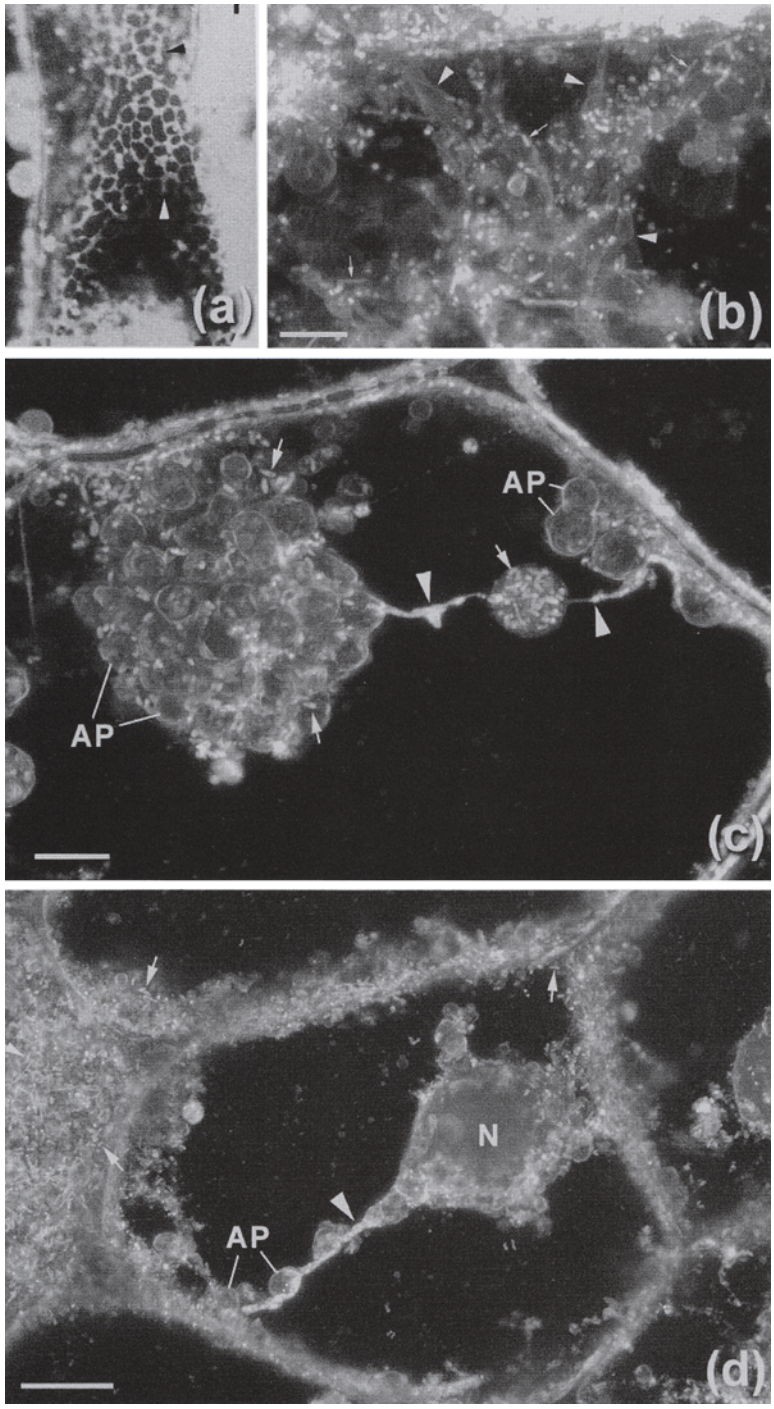

Fig. 2. Cells of symbiotic protocorms of *Spiranthes sinensis* stained with $DiOC_6$ (3) viewed with confocal laser scanning microscopy. (**a**) Cortical ER (arrowhead) forming a network of tubular and cysterna forms in an uncolonized cell. Tissue fixed with 1% glutaraldehyde (GA)-4% paraformaldehyde (PA) in PME (pipes buffer, $MgSO_4$, EGTA). Bar = 10 μm. (**b**) Cortical region of an uncolonized cell. Tubular ER (arrowheads) extends from the cortical ER network to the interior of the cell. Mitochondria (arrows) are associated with the ER. Tissue was fixed in 1% GA-4% PA in PME. Bar = 10 μm. (**c**) Uncolonized cell with ER (arrowheads), mitochondria (arrows), and numerous amyloplasts (AP). Tissue fixed in 1% GA-4% PA in CC (cacodylate buffer, $CaCl_2$). Bar = 10 μm. (**d**) Uncolonized cell focussed to show the nucleus (N). ER (arrowhead) is within a cytoplasmic channel. Amyloplasts (AP) and numerous mitochondria (arrows) are present. Bar = 25 μm.

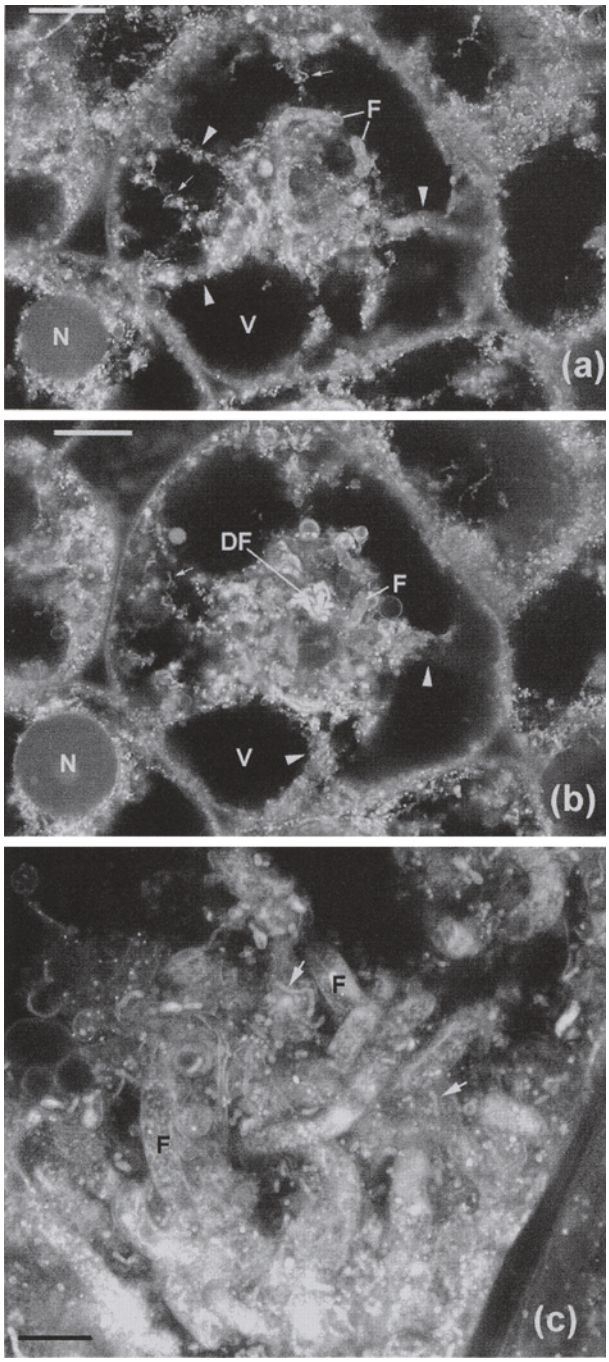

Fig. 3. Colonized cells of *Spiranthes sinensis* protocorms stained with $DiOC_6$ (3) viewed with confocal laser scanning microscopy. (**a**) and (**b**) Two images from different optical sections of a colonized cell. Fungal hyphae (F) and a degenerated hyphal mass (DF) were surrounded by ER. Cytoplasmic channels (arrowheads) connect the peripheral cytoplasm to the cytoplasm surrounding fungal hyphae. Mitochondria (small arrows) are evident in these channels. V=vacuole; N=host cell nucleus. Tissue fixed in 2% GA-2% PA in CC. Bars=25 μm. (**c**) Portion of a colonized cell. Numerous profiles of ER and mitochondria (arrows) are localized around fungal hyphae (F). Tissue fixed in 2% GA-2% PA in CC. Bar=10 μm.

rounded by stained materials (Figs. 3a, 3b).

Distribution of actin filaments Immunolabelling of uncolonized protocorm cells revealed a cortical network of Afs and bundles as well as nucleus-associated Afs (Fig. 4a). Colonized cells retained cortical and nuclear Afs but also had Afs associated with fungal hyphae and degenerated hyphal masses (Fig. 4b). The pre-embedding immunolocalization method for actin filaments gave very specific labelling with virtually no non-specific labelling (Fig. 5a). Control sections using colloidal gold-secondary antibody alone showed no background labelling (not shown). Distribution of gold particles indicated that actin filaments were often the sites of labelling (Figs. 5a, 5c). Actin filaments were localized adjacent to profiles of ER (Figs. 5a, 5b) and mitochondria (Fig. 5b).

Colonized cells with hyphae surrounded by a perifungal membrane had profiles of ER distributed in regions adjacent to the hyphae (Fig. 5d); Afs, as indicated by sites of labelling, also were found in this region of the cell. Collapsed and degenerating peloton hyphae surrounded by an interfacial matrix material and perifungal membrane also had actin filaments and ER located adjacent to the membrane (Fig. 5e).

Discussion

We have shown previously, using various fluorescence techniques combined with CLSM, that both components (Mts and Afs) of the cytoskeletal system of orchid protocorm cells are altered as cells are colonized by fungal hyphae (Uetake et al., 1997; Uetake and Peterson, 1997). In addition, the patterns of Mt reorganization determined by these methods were confirmed using immunocytochemistry at the TEM level and by morphometric analysis of tissues processed for conventional TEM (Uetake and Peterson, 1998). In this latter study, a close association was shown between Mts and the perifungal membrane formed around pelotons and clumps of senescent hyphae. A previous study using various affinity methods at the TEM level (Peterson et al., 1996) had shown the complex nature of the interfacial region between the fungal hyphae and the host cell cytoplasm, and the suggestion was made that Mts may play a role in the organization of this interface (Uetake et al., 1997). The close proximity of cellular organelles to intracellular hyphae in colonized protocorm cells was demonstrated using conventional TEM by Uetake et al. (1992).

The advantage of using a fluoresecent probe, in this case $DiOC_6$ (3), combined with CLSM is evident from the images obtained for distribution of mitochondria and ER in uncolonized and colonized cells in this study. Similar images at the TEM level would require serial sectioning and the laborious reconstruction of the three-dimensional distribution of these organelles. Previous studies using this fluorescent probe with living plant cells have shown that the dynamics of the ER system can be tracked (Knebel et al., 1990; Menzel, 1994; Quader and Schnepf, 1986). Although it was impossible to make similar observations with the complex symbiotic system

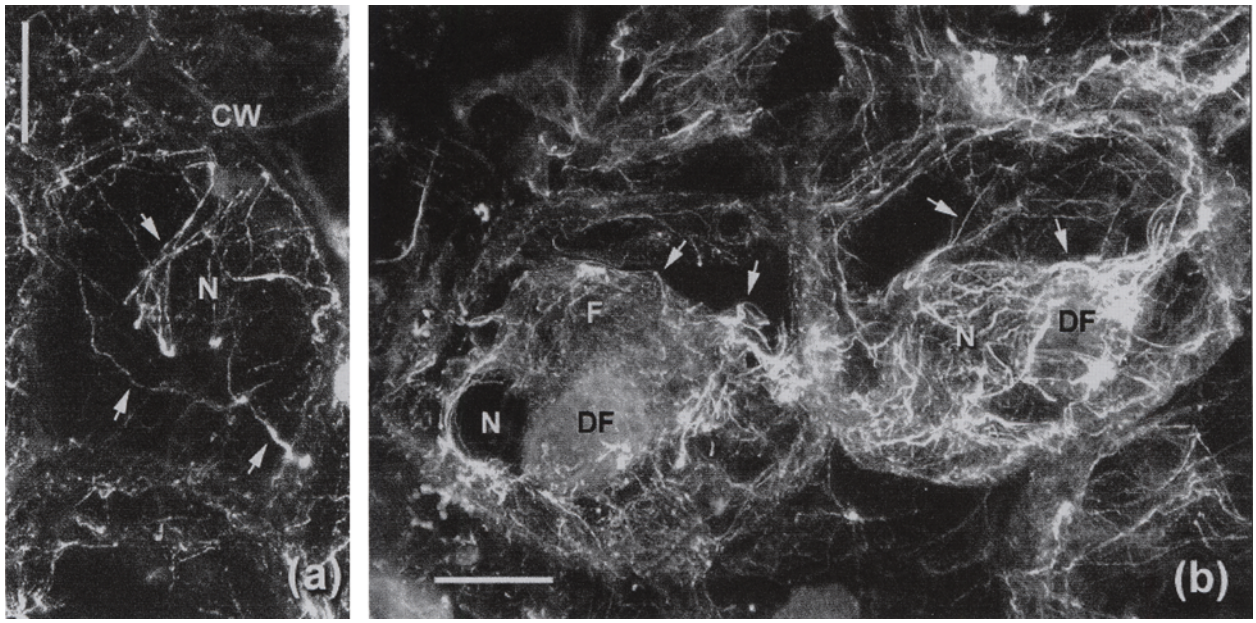

Fig. 4. Uncolonized (**a**) and colonized (**b**) cells of *Spiranthes sinensis* labelled for actin filaments and viewed with confocal laser scanning microscopy. (**a**) Uncolonized cell with a network of actin filaments (arrows), some associated with the nucleus (N). CW=cell wall. Bar=25 μm. (**b**) Colonized cells with fungal hyphae (F) and degenerated hyphae (DF). Actin filaments and bundles (arrows) are associated with fungal hyphae, degenerated hyphae and the cell nucleus (N). Bar=25 μm.

studied here, our observations made on tissue that had been fixed showed that polygonal networks of cortical ER were apparent in colonized and uncolonized cells, and that these were similar morphologically to those reported for living epidermal cells of onion (*Allium cepa* L.) bulb scales (Knebel et al., 1990) and tobacco (*Nicotiana tabacum* L.) leaves (Boevink, et al., 1998). Mild fixation has been reported to have minimal effect on the organization of the cortical ER network in tobacco leaf cells (Boevink et al., 1998), and as shown previously (Terasaki et al., 1984), $DiOC_6$ (3) localized ER in both fresh and fixed tissues. We are, therefore, confident that our observations are not artefactual. The tubular ER with many associated mitochondria observed in the uncolonized protocorm cells probably bridges between the cortical ER and the nucleus and other cytoplasmic domains; the close association between this ER and mitochondria is consistent with TEM observations (Lichtscheidl et al., 1990).

The cytoplasmic channels that bridge between the centrally developing hyphal coil (peloton) and the peripheral cytoplasm in colonized protocorm cells were rich in mitochondria and profiles of cytoplasmic ER. This matches the pattern of Afs in this same system observed here and previously (Uetake and Peterson, 1997) and suggests a close association among these cytoplasmic entities. Staehelin (1997) discusses in detail the complexity in the organization of the ER system in plant cells and summarizes the associations between the ER and other subcellular structures, whereas Reuzeau et al., (1997) discuss a model for the organization of the endomembrane system which includes f-actin as one of the cytoskeletal components ensheathing this membranous system. Our observations of the association between ER and Afs from CLSM and TEM are consistent with previous findings.

Evidence for associations between Afs and ER in plant cells has come from TEM studies (Forde and Steer, 1976; Goosen-De Roo et al., 1983; Hepler et al., 1990; Lichtscheidl and Url, 1990) and, most recently, from studies using fluorescent probes combined with CLSM (Boevink et al., 1998).

Few studies, however, have included immunogold labelling for actin in plant tissues (Lancelle and Hepler, 1989; Lichtscheidl and Url, 1990) and this method has been used infrequently to show ER-Af interactions (Hepler et al., 1990; Lichtscheidl and Url, 1990). Actin filaments are more difficult to localize than Mts using conventional methods of tissue preparation for TEM and, therefore, it has been difficult to correlate our CLSM observations of the distribution of Afs in uncolonized and colonized orchid protocorm cells (this study; Uetake and Peterson, 1997) with the distribution of other organelles using conventional TEM. The results of this study, in which a pre-embedding method for immunogold labelling was used to localize Afs at the TEM level, indicate that these components of the cytoskeletal system are associated with ER and other organelles in both uncolonized and colonized protocorm cells. As far as we are aware, this is the first report of immunogold labelling of Afs in aldehyde-fixed plant tissues combined with a pre-embedding method. It has been demonstrated recently with CLSM that Afs are closely associated with the ER and Golgi in tobacco leaf cells (Boevink et al., 1998), and Reuzeau et al. (1997) review the evidence for ER-Af associations using information gained from studies of epidermal cells of the onion bulb scale.

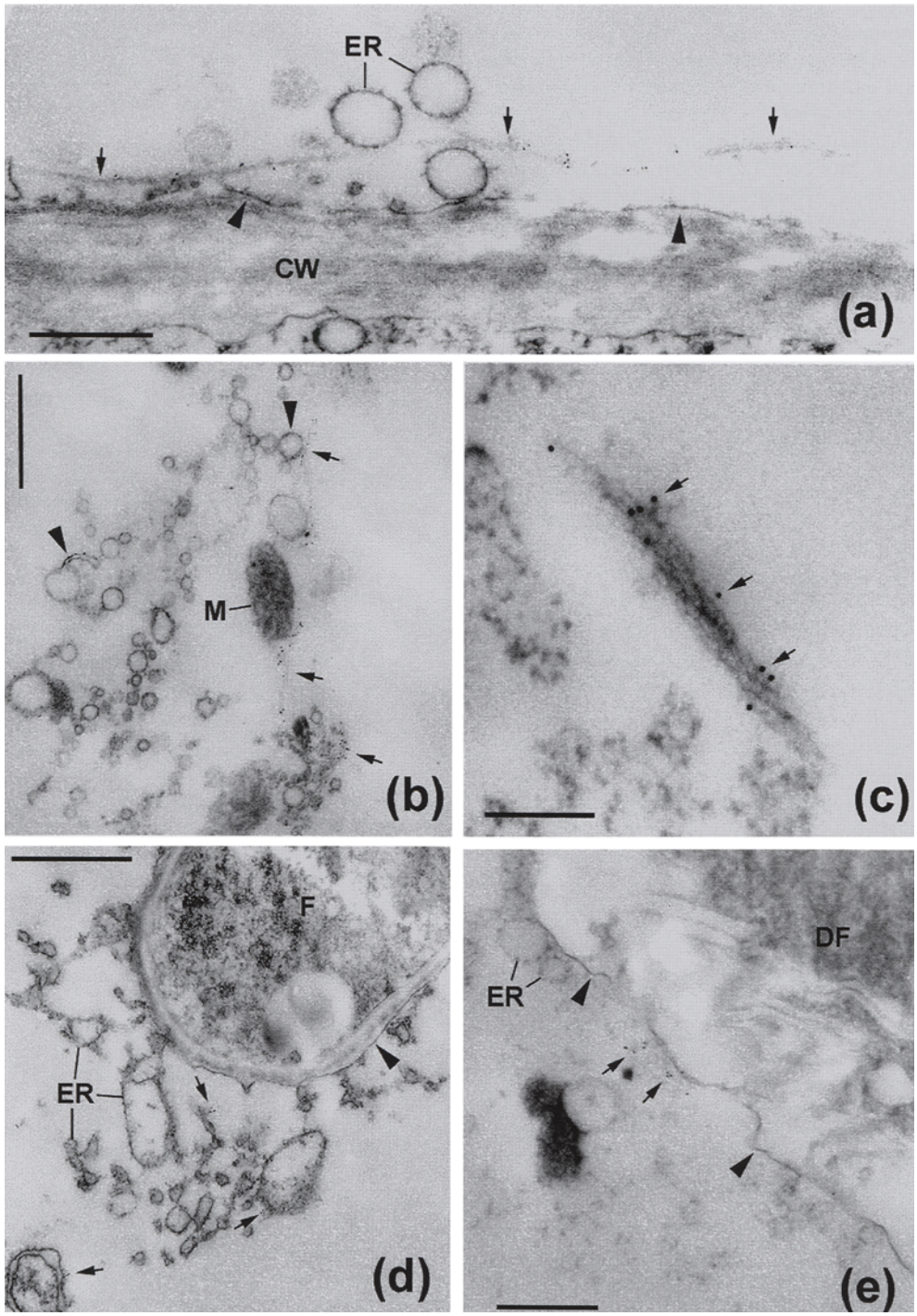

Fig. 5. Transmission electron microscopy of immunogold labelling of actin in protocorm cells of *Spiranthes sinensis*. (a) Gold particles along microfilament bundles (arrows) adjacent to endoplasmic reticulum (ER), both close to the plasma membrane (arrowheads) in an uncolonized cell. CW = Cell wall. Bar = 0.5 μm. (b) Actin filaments (arrows) are evident in the cortical region of an uncolonized cell adjacent to profiles of ER (arrowheads) and a mitochondrion (M). Bar = 1 μm. (c) Actin filaments (arrows) in the cortical cytoplasm. Bar = 0.2 μm. (d) & (e) Immunogold labelling of actin in colonized cells of symbiotic protocorms. (d) Portion of fungal hypha (F) with profiles of endoplasmic reticulum (ER) and actin filaments (arrows) in the cytoplasm adjacent to the hyphae. Arrowhead = perifungal membrane. Bar = 1.0 μm. (e) The periphery of a clump of degenerated hyphae (DF) with a perifungal membrane (arrowheads). An actin filament (arrows) is present close to the perifungal membrane. ER = endoplasmic reticulum. Bar = 0.5 μm.

Our previous results with the orchid protocorm system indicated that Mts are associated closely with the perifungal membrane (Uetake et al., 1997; Uetake and Peterson, 1998), whereas Afs seemed to be more loosely organized around pelotons and collapsed hyphal masses (Uetake and Peterson, 1997). This can perhaps be explained if Afs are linked with the ER surrounding invading hyphae, whereas Mts are attached directly to the perifungal membrane. The present results indicate that ER and Afs may be closely associated with the perifungal membrane surrounding peloton hyphae and clumps of senescent hyphae, but this requires further confirmation. Ultrastructural studies of biotrophic pathogenic fungi have shown a close association between ER and the host membrane that surrounds the haustorium (Hickey and Coffey, 1977; Harder et al., 1978). A recent approach that has been particularly successful in showing a close relationship between ER and the extrahaustorial membrane in pea (*Pisum sativum* L.) leaf cells infected by the biotrophic pathogenic fungus *Erysiphe pisi*, involved an ER-specific anti-HDEL monoclonal antibody (Leckie et al., 1995). Approaches such as this are worth consideration for further studies of the interface that forms for bidirectional nutrient exchange in endomycorrhizal associations. It is probable that the cytoplasmic environment immediately adjacent to biotrophic fungal hyphae within plant cells is far more complex than that visualized to date.

Acknowledgements——This research was supported by the Natural Sciences and Engineering Research Council of Canada. We thank John Greenwood for advice on immunolabelling and Melissa Farquhar for her continued help with confocal microscopy.

Literature cited

Baluška, F., Bacigálová, K., Oud, J. L., Hauskrecht, M. and Kubica, Š. 1995. Rapid reorganization of microtubular cytoskeleton accompanies early changes in nuclear ploidy and chromatin structure in postmitotic cells of barley leaves infected with powdery mildew. Protoplasma **185**: 140–151.

Boevink, P., Opaka, K., Santa Cruz, S., Martin, B., Betteridge, A. and Hawes, C. 1998. Stacks on tracks: the plant Golgi apparatus traffics on an actin/ER network. Plant J. **15**: 441–447.

Bonfante, P., Bergero, R., Xavier, U., Romera, C., Rigau, J. and Puigdomenech, P. 1996. Transcriptional activation of a maize α-tubulin gene in mycorrhizal maize and transgenic tobacco plants. Plant J. **9**: 737–743.

Forde, J. and Steer, M. W. 1976. Cytoplasmic streaming in *Elodea*. Can. J. Bot. **54**: 2688–2694.

Genre, A. and Bonfante, P. 1997. A mycorrhizal fungus changes microtubule orientation in tobacco root cells. Protoplasma **199**: 30–38.

Genre, A. and Bonfante, P. 1998. Actin versus tubulin configuration in arbuscule-containing cells from mycorrhizal tobacco roots. New Phytol. **140**: 745–752.

Goosen-De Roo, L., Burggraaf, P. D. and Libbenga, K. R. 1983. Microfilament bundles associated with tubular endoplasmic reticulum in fusiform cells in the active cambial zone of *Fraxinus excelsior* L. Protoplasma **116**: 204–208.

Harder, D. E., Rohringer, R., Samborski, D. J., Kim, W. K. and Chong, J. 1978. Electron microscopy of susceptible and resistant near-isogenic (sr6/Sr6) lines of wheat infected by *Puccinia graminis* tritici. The host-pathogen interface in the compatible (sr6/P6) interaction. Can. J. Bot. **56**: 2955–2966.

Hardham, A. R. and Mitchell, H. J. 1998. Use of molecular cytology to study the structure and biology of phytopathogenic and mycorrhizal fungi. Fungal Genet. Biol. **24**: 252–284.

Heath, M. C. 1997. Signalling between pathogenic rust fungi and resistant or susceptible host plants. Ann. Bot. **80**: 713–720.

Hepler, P. K., Palevitz, B. A., Lancelle, S. A., McCauley, M. M. and Lichtscheidl, I. 1990. Cortical endoplasmic reticulum in plants. J. Cell Sci. **96**: 355–373.

Hickey, E. L. and Coffey, M. D. 1977. A fine-structural study of the pea downy mildew fungus *Peronospora pisi* on its host *Pisum sativum*. Can. J. Bot. **55**: 2845–2858.

Knebel, W., Quader, H. and Schnepf, E. 1990. Mobile and immobile endoplasmic reticulum in onion bulb epidermis cells: short- and long-term observations with a confocal laser scanning microscope. Eur. J. Cell Biol. **52**: 328–340.

Kobayashi, I., Kobayashi, Y. and Hardham, A. R. 1994. Dynamic reorganization of microtubules and microfilaments in flax cells during the resistance response to flax rust infection. Planta **195**: 237–247.

Kobayashi, I., Kobayashi, Y., Yamamoto, N. and Kunoh, H. 1992. Recognition of a pathogen and a nonpathogen by barley coleoptile cells. III. Responses of microtubules and actin filaments in barley coleoptile cells to penetration attempts. Can. J. Bot. **70**: 1815–1823.

Kobayashi, I., Murdoch, L. J., Kunoh, H. and Hardham, A. R. 1995. Cell biology of early events in the plant resistance response to infection by pathogenic fungi. Can. J. Bot. **73** (Suppl. 1): S418–S425.

Kobayashi, Y., Kobayashi, I., Funaki, Y., Fujimoto, S., Takemoto, T. and Kunoh, H. 1997a. Dynamic reorganization of microfilaments and microtubules is necessary for the expression of non-host resistance in barley coleoptile cells. Plant J. **11**: 525–537.

Kobayashi, Y., Yamada, M., Kobayashi, I. and Kunoh, H. 1997b. Actin microfilaments are required for the expression of nonhost resistance in higher plants. Plant Cell Physiol. **38**: 725–733.

Lancelle, S. A. and Hepler, P. K. 1989. Immunogold labelling of actin on sections of freeze-substituted plant cells. Protoplasma **150**: 72–74.

Leckie, C. P., Callow, J. A. and Green, J. R. 1995. Reorganization of the endoplasmic reticulum in pea leaf epidermal cells infected by the powdery mildew fungus *Erysiphe pisi*. New Phytol. **131**: 211–221.

Lichtscheidl, I. K., Lancelle, S. A. and Hepler, P. K. 1990. Actin-endoplasmic reticulum complexes in *Drosera*. Their structural relationship with the plasmalemma, nucleus, and organelles in cells prepared by high pressure freezing. Protoplasma **155**: 116–126.

Lichtscheidl, I. K. and Url, W. G. 1990. Organization and dynamics of cortical endoplasmic reticulum in inner epidermal cells of onion bulb scales. Protoplasma **157**: 203–215.

Matsubara, Y., Uetake, Y. and Peterson, R. L. 1999. Entry and colonization of *Asparagus officinalis* roots by arbuscular mycorrhizal fungi with emphasis on changes in host microtubules. Can. J. Bot. **77**: 1159–1167.

Menzel, D. 1994. Dynamics and pharmacological perturbations of the endoplasmic reticulum in the unicellular green alga *Acetabularia*. Eur. J. Cell Biol. **64**: 113–119.

Peterson, R. L., Bonfante, P., Faccio, A. and Uetake, Y. 1996. The interface between fungal hyphae and orchid protocorm cells. Can. J. Bot. **74**: 1861–1870.

Peterson, R. L., Uetake, Y. and Armstrong, L. N. 1999. Interactions between fungi and plant cell cytoskeleton. In: Current advances in mycorrhizae research, (ed. By Podila, G. K. and Douds, D. D. Jr.), pp. 157–178. APS Press, St. Paul.

Peterson, R. L., Uetake, Y. and Zelmer, C. 1998. Fungal symbioses with orchid protocorms. Symbiosis **25**: 29–55.

Quader, H., Hofmann, A. and Schnepf, E. 1987. Shape and movement of the endoplasmic reticulum in onion bulb epidermis cells: possible involvement of actin. Eur. J. Cell Biol. **44**: 17–26.

Quader, H. and Schnepf, E. 1986. Endoplasmic reticulum and cytoplasmic streaming: fluorescence microscopical observations in adaxial epidermis cells of onion bulb scales. Protoplasma **131**: 250–252.

Reuzeau, C., McNally, J. G. and Pickard, B. G. 1997. The endomembrane sheath: a key for understanding the plant cell? Protoplasma **200**: 1–9.

Škalamera, D. and Heath, M. C. 1998. Changes in the cytoskeleton accompanying infection-induced nuclear movments and the hypersensitive response in plant cells invaded by rust fungi. Plant J. **16**: 191–200.

Staehelin, L. A. 1997. The plant ER: a dynamic organelle composed of a large number of discrete functional domains. Plant J. **11**: 1151–1165.

Terasaki, M., Song, J. D., Wong, J. R., Weiss, M. J. and Chen, L. B. 1984. Localization of endoplasmic reticulum in living and glutaraldehyde fixed cells with fluorescent dyes. Cell **38**: 101–108.

Uetake, Y., Farquhar, M. L. and Peterson, R. L. 1997. Changes in microtubule arrays in symbiotic orchid protocorms during fungal colonization and senescence. New Phytol. **135**: 701–709.

Uetake, Y., Kobayashi, K. and Ogoshi, A. 1992. Ultrastructural changes during the symbiotic development of *Spiranthes sinensis* (Orchidaceae) protocorms associated with binucleate *Rhizoctonia* anastomosis group C. Mycol. Res. **96**: 199–209.

Uetake, Y. and Peterson, R. L. 1997. Changes in actin filament arrays in protocorm cells of the orchid species, *Spiranthes sinensis*, induced by the symbiotic fungus *Ceratobasidium cornigerum*. Can. J. Bot. **75**: 1661–1669.

Uetake, Y. and Peterson, R. L. 1998. Association between microtubules and symbiotic fungal hyphae in protocorm cells of the orchid species, *Spiranthes sinensis*. New Phytol. **140**: 715–722.